RSC Advances

This article can be cited before page numbers have been issued, to do this please use: P. KESHARWANI, A. Jain, A. Jain, A. Jain, N. K. Garg, R. K. Tekade, R. Thakur and A. Iyer, *RSC Adv.*, 2016, DOI: 10.1039/C6RA17290C.

ROYAL SOCIETY OF CHEMISTRY

www.rsc.org/advances

View Article Online
DOI: 10.1039/C6RA17290C

Cationic Bovine Serum Albumin (CBA) conjugated Poly Lactic-co-Glycolic Acid (PLGA) nanoparticles for extended delivery of methotrexate into brain tumor

Prashant Kesharwani,[1*] Ashay Jain,[2] Atul Jain,[2] Amit K Jain,[2] Neeraj Kumar Garg,[2] Rakesh Kumar Tekade,[3] Thakur Raghu Raj Singh[4], Arun K. Iyer[5]

[1] The International Medical University, School of Pharmacy, Department of Pharmaceutical Technology, Kuala Lumpur, 57000, Malaysia
[2] Department of Pharmaceutical Sciences, Dr. Hari Singh Gour University, Sagar, M.P., 470003, India
[3] School of Pharmacy, Department of Pharmaceutical Technology, International Medical University, Jalan Jalil Perkasa 19, 57000 Kuala Lumpur, Malaysia
[4] School of Pharmacy, Queen's University Belfast, Medical Biology Centre, 97 Lisburn Road, Belfast BT9 7BL, UK
[5] Use-inspired Biomaterials & Integrated Nano Delivery (U-BiND) Systems Laboratory, Department of Pharmaceutical Sciences, Eugene Applebaum College of Pharmacy and Health Sciences, 259 Mack Ave, Wayne State University, Detroit, MI 48201, USA

***Address for correspondence**

Dr. Prashant Kesharwani
The International Medical University,
School of Pharmacy,
Department of Pharmaceutical Technology,
Kuala Lumpur, 57000, Malaysia
Email: prashantdops@gmail.com; prashant_pharmacy04@rediffmail.com (P. Kesharwani)

Disclosures: There is no conflict of interest and disclosures associated with the manuscript.

View Article Online
DOI: 10.1039/C6RA17290C

Abstract

Current treatment strategies for the treatment of brain tumor have been hindered primarily by the presence of highly lipophilic insurmountable blood-brain barrier (BBB). The purpose of current research was to investigate the efficiency of engineered biocompatible polymeric nanoparticles (NPs) as drug delivery vehicle to bypass the BBB and enhance biopharmaceutical attributes of anti-metabolite methotrexate (MTX) encapsulated NPs. The NPs were prepared by solvent diffusion method using cationic bovine serum albumin (CBA), and characterized for physicochemical parameters such as particle size, polydispersity index, and zeta-potential; while the surface modification was confirmed by FTIR, and NMR spectroscopy. Developed NPs exhibited zestful relocation of FITC tagged NPs across BBB in albino rats. Further, hemolytic studies confirmed them to be non-toxic and biocompatible as compared to free MTX. *In vitro* cytotoxicity assay of our engineered NPs on HNGC1 tumor cells proved superior uptake in tumor cells; and elicited potent cytotoxic effect as compared to plain NPs and free MTX solution. The outcomes of the study evidently indicate the prospective of CBA conjugated poly (D,L-lactide-co-glycolide) (PLGA) NPs loaded with MTX in brain cancer bomber with amplified capability to circumvent BBB.

Keywords: Poly (D,L-lactide-co-glycolide); Nanoparticles; Methotrexate; Cationic bovine serum albumin; Brain targeting; Brain tumor.

View Article Online
DOI: 10.1039/C6RA17290C

1. Introduction

Brain tumors constitute a solicitous and unsolved problem in the treatment because of inadequacy in bypassing the blood brain barrier (BBB)[1,2] and mitigation of brain tumor is still the foremost challenging obligation[3]. BBB, a highly lipophilic barrier consist of the vascular structures composed of physical obstacle (tight junctions of astrocytes and endothelial cells), and well organised traffic controller of the metabolic barriers (multidrug resistance (MDR) pathways), that is managing the transport of bioactive materials across the BBB [4–7]. The Cassette transport pump (p-glycoprotein) shows fundamental role in the drug efflux at the level of BBB [8]. However, hydrophobic small molecular drugs can be easily transported across the BBB; and diverse attempts have been made to transport active molecules across the BBB [9,10]. The successful management of brain tumor necessitates the bypassing, inactivate or suppress the metabolic BBB barriers [11]. Therefore, expansion of an efficient system to bear the active molecules across the BBB has been a major challenge in research and stress must therefore be resolute on developing approach that enhances the bioavailability in the central nervous system (CNS).

Nanotechnology indeed exploited in the most of the pharmacological complication of active molecules that results in increment in their therapeutic efficiency [12–15]. Biocompatible nanostructured systems confess the interactions with biomolecules and interior environment of the cell and may sidestep the highly lipophilic physical obstacle that limits the passage of wide verity of therapeutic agent across BBB [16–18]. Nowadays surface engineering of nanocarriers for target specific delivery of active molecules have been considered a viable strategy for the improved therapeutic efficacy in the management of brain tumor[19–22]. Thus, targeting strategies are capable of crossing barriers present in BBB to overcome the limited transport across it. Out of various approaches, adsorptive transcytosis via cationic bovine serum albumin (CBA) has been scrutinize to bypass BBB without influencing the integrity of tight junction at BBB [23–25]. Surface modification of NPs finesses the BBB via adsorptive transcytosis where interaction between BSA and cell membrane) at the BBB demonstrate BSA preferentially encourage transport of nanocarriers across BBB [26–29].

Methotrexate (MTX), a dihydrofolate reductase (DHFR) inhibitor acting in S-phase of the cell cycle plays a crucial role in the treatment of brain cancer by introducing itself within the folate stacks[30,31]. However, the inability to deliver MTX across BBB owing to its hydrophilic

View Article Online
DOI: 10.1039/C6RA17290C

nature and the distribution of the drug at noncancerous sites has severely compromised its clinical application. Therefore, nanostructured drug delivery vehicles, which are able to bypass BBB and cell membranes of brain tumor cells is an urgent and inevitable requirement for the treatment of brain tumors. United States Food and Drug Administration (US-FDA) approved the biodegradable non-immunogenic, biocompatible polyester polymers such as poly (D,L-lactide-co-glycolide) (PLGA) in targeted drug delivery of drugs for various ailments[32–35].

The prepared NPs formulation engineered with CBA was physico-chemically characterized and evaluated using *in vitro*, *ex vivo* (cell line) and *in vivo* studies. Moreover, a comparative study of brain uptake of FITC tagged NPs following intravenous injection was confirmed by fluorescence microscopy. In nutshell, the present study with CBA modifiedPLGA-NPs encapsulated MTX opens new horizon not only to understand the difficulties but also improvement in management of effective treatment of brain cancer.

2. Materials, methods and Instrumentation

2.1. Materials

MTX, bovine serum albumin (BSA), 1-ethyl-3-(3-dimethylaminopropyl) carbodiimide and (EDC) were purchased from Sigma Aldrich (Germany). PLGA, 50:50), N-hydroxy succinimide (NHS), Di-methyl-sulphoxide (DMSO), PluronicF-68(PF-68), FITC, Triton-X100 were purchased from Himedia, Mumbai, India. Nylon membrane filter (0.22 μm) was purchased from Pall Gelman Sciences (USA). All other reagents and solvents were of analytical grade unless otherwise specified. Ultra-pure deionized water was used through the study.

2.2. Preparation of cationic bovine serum albumin (CBA)

CBA was prepared from BSA following the well-established procedure reported earlier with trivial modifications (Feng *et al.,* 2009). Briefly, 0.5 g of BSA was treated with little exceeding of ethylenediamine (EDA) previously solubilised in conjugation buffer (MES; 0.2 mol/L) at 4±1 °C while being agitate using magnetic stirrer (Remi, India) and the pH was adjusted to 4.7. Supplementary, 50 mg of 1-ethyl-3-(3-dimethylaminopropyl) carbodiimide (EDC) was added and allowed to keep undisturbed for 2 h in dark, at ambient temperature. The reaction was continued by addition of 0.4 ml of acetate buffer (2 mol/L; pH 4.75). Finally, the solution was dialyzed extensively against ultrapure deionised water for 48 h, lyophilized and stored in hermetically sealed container. Further, BSA and CBA were further characterized using NMR (Bruker DRX, USA) and FTIR spectroscopy (Perkin-Elmer, USA).

View Article Online
DOI: 10.1039/C6RA17290C

2.3. Fabrication of nanoparticles

The MTX loaded PLGA NPs were prepared in accordance to the solvent-diffusion technique described by Song *et al.*, 2006 [36] with slight modifications. Briefly, MTX was dissolved in PBS (pH 7.4)/DMSO. Subsequently, aqueous solution of Pluronic® F-68 (PF-68) (PBS; pH 7.4) was added as a stabilizer to the drug solution. To it 1% w/v PLGA solution (the organic phase; 10 ml) in ethyl acetate was added drop-wise into 20 ml of an aqueous phase consisting drug and stabilizer under regular magnetic agitation (REMI Instrument India). This pre-emulsion was maintained above the melting temperature using a hot water bath and the stirring of high speed was set out to attain a pre-emulsion phase followed by sonication. In addition, a measured volume of ultra-pure deionized water was supplied to the o/w emulsion under gentle stirring to facilitate the diffusion of organic phase into an aqueous solvent leading to the formation of MTX loaded PLGA NPs (MTX-NPs). Subsequently, NPs dispersion was filtered through 0.22 μm membrane filters. Finally, the MTX-NPs dispersion was lyophilized (Heto Drywinner, Denmark, Germany) and stored for further studies. FITC labeled NPs were prepared by co-encapsulation of FITC along with MTX in PLGA NPs.

2.4. Fabrication of CBA conjugated MTX loaded PLGA NPs (CBA-MTX-NPs)

Freeze dried MTX-NPs were dispersed in ultra-pure deionized water at a concentration of 20 mg/ml. Subsequently, 50 mg N-hydroxy succinimide (NHS) was added and allowed to be agitated for next 6 h followed by addition of EDC (15 mg) while constant stirring (Magnetic stirrer; Remi, India) for 48 h at ambient temperature. Afterwards, CBA (50 mM) was added while agitating all night (2000 rpm) to facilitate its conjugation with the MTX-NPs. The dispersion was then finally dialyzed against ultra-pure deionized water for 30 min to take away free CBA and other impurities followed by lyophilization (Heto Drywinner, Denmark, Germany).

2.5. Characterization of nanoparticles

2.5.1. Measurement of particle size and zeta potential

The average particle size and poly dispersity index (PDI) of MTX-NPs and CBA-MTX-NPs was determined by a Zetasizer (DTS ver. 4.10, Malvern Instruments, England). Briefly, nano-particulate sample dispersion was added in polystyrene cuvettes diluted with ultra-pure deionized water and analyzed at a 90° fixed angle. The zeta potential of NPs formulation was measured by determining electrophoretic mobility with a laser-based multiple angle particle

View Article Online
DOI: 10.1039/C6RA17290C

electrophoresis analyzer, Malvern Zetasizer (DTS Ver. 4.10, Malvern Instruments, England). The nanoparticles were suspended in ultra-pure de-ionized water and kept in an electrophoretic cell with an electric field of 15.24 V/cm and the zeta potential was measured.

2.5.2. Scanning electron microscopy

Surface morphology was determined by scanning electron microscope (SEM). In brief, the NPs powder was sprinkled on a double adhesive tape which was stuck on an aluminium stub. Following this the stubs were coated with gold at a thickness of about 300 Å by using a sputter coater. All NPs and examined under a SEM (LEO 435 VP, Eindhoven Netherlands) at an acceleration voltage of 30 kV and photographs were taken at various magnifications.

2.5.3. Encapsulation efficiency

The drug encapsulation efficiency was estimated using a dialysis method for separating unloaded MTX from the NPs. This was then analyzed spectrophotometrically to indirectly determine the amount of drug bound with the NPs. Momentarily, 5 ml of the MTX-NPs dispersion was placed into a dialysis bag (MWCO 1000 KDa, Himedia, India) and dialyzed against 50 ml of 0.1N NaOH for 60 minutes with magnetic stirring (50 rpm). Samples (0.5 ml) were withdrawn occasionally and collected into HPLC vials (Himedia, India) until no drug was detected in the receptor compartment[37]. All samples (injection volume – 10µl) were quantified for MTX content by HPLC at a flow rate of 1ml/min at 302 nm and at 40°C. Samples were loaded into the HPLC system to quantify the unentrapped amount of MTX, so as to quantify indirectly the amount of entrapped MTX within theNPs[38–40]. The same exercise was carried out to measure the entrapped drug in CBA conjugated NPs and the quantification was performed using HPLC (Shimadzu, Japan). The reversed phase C_{18} column (4.6 mm×250 mm, 5µm) was used for chromatographic separation. The mobile phase was a mixture of buffer (pH 6.0) and acetonitrile at a ratio of 9:1. The buffer consisted of 0.12 M di-sodium hydrogen orthophosphate and 0.03 M citric acid. [41].

2.6. *In vitro* release study

The ability of NPs to release drugs into external media was determined by conducting the *in vitro* drug release assay on the developed NPs. The dialysis tube diffusion technique was used to estimate *in vitro* release of MTX from MTX-NPs and CBA-MTX-NPs. The fixed volume of the prepared nano-particulate formulations (5 ml) were poured into the dialysis tubing (MWCO 1000 KDa), tied at both ends and immersed into receptor media consisting 100 ml of phosphate

View Article Online
DOI: 10.1039/C6RA17290C

buffer saline pre-equilibrated at 37±2°C followed by moderate stirring (magnetic stirring;100 rpm). 0.5 ml sample from recipient compartment was withdrawn intermittently and an equal quantity of fresh medium was added after each sample withdrawal in a receptor compartment to maintain a constant sink volume over the experiment. The same practice was adopted for the determination of drug release profile at pH 5.4 (mimicking acidic tumor environment). Samples were analyzed by HPLC using same method described above and the amount of MTX released over time was quantified[41,42].

2.7. *Ex vivo* study

2.7.1. Cytotoxicity Study

Human brain cancer cell lines (C6 glioma) was purchased from the National Center for Cell Sciences (NCCS), Pune, India; and cultured in DMEM (Dulbecco's Modified Eagle's Medium; Himedia, India) supplemented with 10%v/v heat-inactivated fetal bovine serum (FBS), 1%v/v streptomycin, 3 mM glutamine in a 37±2°C humidified incubator and 5% CO_2 atmosphere. Cytotoxicity of NPs was evaluated by sulforhodamine B (SRB) staining assay [43]. This assay is based on measurement of optical density for the determination of cell survival and proliferation. Principally this assay determines the metabolic activity of viable cells. Exponentially growing C6 glioma cells were plated at a density of 7×10^4 cells/ml in 24 well plates (Sigma, Germany). The cells were then incubated with predetermined concentrations (100.0–0.01 μM) of MTX (free MTX; MTX-NPs, CBA-MTX–NPs and CBA [1 mg/ml]+ CBA-MTX–NPs) under restricted environment for 72 h. Afterwards, 20μl of cold trichloroacetic acid (TCA; 50%) was added to each well and kept undisturbed for an hat 4°Cto facilitate cell fixation. Subsequently, the plates were rinsed with ultra-pure deionized water, dried and stained with 50-60 μl of 5%w/v SRB reagent (constructed in 1%v/v acetic acid) for an h. Then, 150 μl of acetic acid was aspirated to remove the excess of SRB reagent. In each well, TRIS was added and well-mixed on a shaker for few minutes. The optical density (OD) of each well was then measured at 490 nm via microplate spectrophotometer (Model 680, Bio-Rad, Japan).

2.7.2. Cellular uptake assay

Cellular uptake efficiency of NPs was evaluated as a function of ligand using fluorescence activated cell sorters (FACS) instrument (BD Biosciences FACS Aria, Germany) againstC6 glioma cells. Glioma cells were cultured in accordance with the process described under cytotoxicity studies. Briefly, cells were seeded in 6 well plates (Sigma, Germany) at a

View Article Online
DOI: 10.1039/C6RA17290C

2×10^6 cells/ml using fresh culture medium and allowed to suspend for 12 h in humidified incubator at 37±2°C with 5% CO_2 atmosphere. Cellular internalization of different dose of MTX formulation was determined by *in vitro* incubation of cells with fluorescein isothiocyanate (FITC), FITC labeled NPs and CBA [1mg/ml]+ CBA conjugated FITC labeled NPs in separate wells for 1 h. NPs which were adhered to the cell surface were detached by washing each well twice with PBS (pH ~7.4). Further, cells were trypsinized (0.1% w/v), kept for 5 min, and harvested by adding 1 ml PBS (pH ~7.4) followed by probe sonication for five times to obtain the cell lysate. Finally, cell lysate was centrifuged at 12,000 rpm for 10 min, and the supernatant was subjected to florescence assay using FACS. Same procedure was followed to study the cellular uptake profile after 2 and 6 h [3,44].

2.8. *In vivo* pharmacokinetic and biodistribution studies

The *in vivo* validation of the developed formulation (MTX-NPs and CBA-MTX-NPs) was performed to evaluate the CBA mediated transport while bypassing the BBB, and drug distribution in various organs of Balb/c mice (20–25 g; either sex). All animal experimentation procedures were carried out with prior permission and approval by Institutional Animals Ethical Committee, Dr. Hari Singh Gour University, Sagar (M.P.; India). The animals were fasted all the night with free access to water ad libitum. A short incision was made through the skin to expose the cranium and approximately 6×10^5 C6 glioma cells/10 µl in serum-free 2%v/v DMEM were stereotaxically rooted into the right forebrain of each animal[45].

Previously weighed tumor bearing animals were randomly divided into four groups of nine animals each. MTX, MTX-NPs and CBA-MTX-NPs were dispersed in normal saline. The formulations were administered at a dose of 5.0 mg/kg body weight through the lateral tail vein of animals of first, second and third groups, respectively[46]. Animals of fourth group served as a control for this study. Approximately 300 µl blood samples were withdrawn from retro-orbital plexus under mild anesthesia at 0.16, 0.5, 1.0, 2.0, 3.0, 5, 8, 12, 18, 21 and 24 h intervals in heparinized tubes. Blood samples were collected from three animals of each group and were assassinated by cervical dislocation after the study.

The organs viz. brain, liver, kidney, heart spleen and tumor were isolated carefully, weighed and stored at −80 °C until experimentation. Afterwards, blood sample was collected from other three animals *(n = 6)* of each group for 2–8 h intervals, euthanized and different

View Article Online
DOI: 10.1039/C6RA17290C

organs were isolated. This exercise was also repeated for last three animals of each group for 8–24 h intervals.

Plasma was separated from blood samples by centrifugation at 10,000 rpm for 15 min. Afterwards, 100 µl of plasma was filtered into micro-centrifuge tube and same quantity of acetonitrile was added to precipitate the protein.

At the same time, the organs were chopped and homogenized to detach the tissues, vortexed for one minute, and kept undisturbed for 30 min. Tissue homogenates were then treated with100 µl of acetonitrile. Further, the serum and tissue homogenates earlier admixed with acetonitrile were vortexed for 1 min, and subsequently centrifuged at 5000 rpm for 15 min. The supernatant was filtered through a 0.22 µm syringe filter, collected in HPLC vials (Himedia, India), and quantified for MTX content. Quantification of MTX was done in serum as well as in various tissues *viz.* brain (glioma cells), heart, liver, spleen and kidney was performed by HPLC method as described earlier [41,47].

2.9. Hemolytic toxicity

Hemolytic study was performed following the procedure described earlier with slight modifications [39,48]. Briefly, whole human blood samples were collected from a healthy person (with kind consent) and heparinized in HiAnticlot blood collection vials (Himedia, India). Subsequently, the red blood cells (RBCs) suspension was centrifuged and resuspended in normal saline. Two mL of the RBCs suspension was separately dispersed in normal saline solution producing no hemolysis (served as control '0 % hemolysis') and in distilled water considered to be producing 100% hemolysis. One ml of adequately diluted plain MTX solution, MTX-NPs, and CBA–MTX–NPs were incubated individually with 2 ml RBCs suspension and the volume was made up to 10 ml with normal saline.

The formulations were taken in such amount that the resultant final concentration of MTX was equivalent in every case so as to facilitate the assessment of extent of hemolysis followed by effect of tween 80 (Himedia, Mumbai, India) coating on hemolysis. Further, the formulations were allowed to incubate at 37±1 °C for 30 min, followed by centrifugation at 4000 rpm for 10 min. Subsequently, supernatants were taken and diluted with an equal volume of normal saline and absorbance was measured by UV-Visible spectrophotometer (Schimadzu, 1601 Japan) at 540 nm against normal saline diluted similarly as blank. The percent hemolysis

View Article Online
DOI: 10.1039/C6RA17290C

was then determined for each sample by taking absorbance of distilled water which was assumed to be producing 100% hemolysis.

2.10. Data analysis

Statistical analysis of the data was articulated as the mean ± S.D and statistical analysis was computed using one-way analysis of variance (ANOVA) with a Tukey–Kramer multiple comparison Post- test using GraphPad InStat™ software (GraphPad Software Inc., San Diego, California). A probability level of $p<0.05$ was considered to be significant.

3. Results and discussion

3.1. Preparation of CBA

The FTIR spectroscopy of pure BSA (Fig. 1A) shows the distinctive peaks at 3280.16 cm^{-1} (stretching vibration of –OH), 2966.17 cm^{-1} amide (–N-H stretching vibration), 1635.01 cm^{-1}(C=O stretching vibrations), 1515.49 cm^{-1} (coupling of bending vibrate of N–H and stretching vibrate of C–N) cm^{-1}, 1388.88 cm^{-1} (aromatic -C=C-) and 1037.46 cm^{-1} (C–O bending) (Fig. 1A). After cationization discrepancy in the FTIR peaks are understandable with elevated intensity at parallel wavelength because of the presence of auxiliary ethylene amine group in CBA incorporated during cationization. Shifting of FTIR peak of –OH groups, C=O stretching, and disappearance of 1388.88 cm^{-1} (aromatic -C=C-stretching) confirmed the cationization of BSA (Fig. 1B). In NMR spectroscopy, amine group ($-NH_2$) shows high shielding effect and the obtained spectra of CBA illustrated its characteristic peak at 3.5 ppm which confirms the presence of amine group in CBA (Fig. 2A).

3.2. Preparation of CBA conjugated MTX loaded NPs (CBA-MTX-NPs)

The NPs were fabricated by an emulsification-diffusion method and the carboxylic group of NPs was conjugated to amine functionalities of CBA according to a previously reported method as reported earlier with slight modifications [49–51]. This technique involved the quick diffusion of solvent across the solvent–lipid phase into aqueous phase followed by evaporation of solvent leading to enhanced rigidity of the NPs.

Addition of CBA in presence of NHS and EDAC leads to formation of amide (–CONH–) bond between amine ($–NH_2$) groups of CBA and carboxylic acid (–COOH) present on the surface of NPs. Amalgamation of CBA appended NPs was further confirmed by FTIR and NMR spectroscopy. The presence of peaks depicting N–H stretch at 3432.01cm^{-1}, C=O stretching at

View Article Online
DOI: 10.1039/C6RA17290C

1723.95 cm^{-1} and C–O stretching at 1360.42 cm−1 confirmed the amide bond formation, and hence the conjugation between NPs and CBA (Fig. 1C). In NMR Spectra, acidic group (-COOH) demonstrate its peak at deshielded position or away from the reference line of tetra methyl silane in NMR spectra. In NMR spectra of CBA-MTX-NPs, distinguish peak with less intensity at 8.5 ppm indicated that the most of the free carboxylic group get saturated with amine group of CBA, thus confirmed the formation of amide bond between carboxylic groups of MTX-NPs made up of PLGA and amine groups of CBA (Fig. 2 B).

3.3. Characterization of nanoparticles

3.3.1. Size, Zeta Potential and Surface morphology

The average particle size of CBA conjugated MTX-NPs as measured by dynamic light scattering technique was found to be larger than that of unconjugated formulation (Fig. 3 and Table 1). The disparity in the average size may be due to the conjugation of CBA on the surface of MTX-NPs. The average particle size of MTX-NPs was found to be108.3±3.1nm while in case of CBA conjugated formulation it was 120.9±4.4 nm. The mean diameters of NPs were well below 200 nm and these fallouts are in harmony with SEM photographs of the CBA conjugated NPs (Fig. 4A and B).

Zeta potential is an imperative criterion in order to establish the storage stability of nanometric particulate system. The zeta potential of MTX-NPs and CBA-MTX-NPs formulations was found to be -13.7± 0.4 mV and -5.55± 0.3 mV, respectively (Fig. 3 and Table 1). The higher negative magnitude of zeta potential might be ascribed to the –COO (carboxylic) group exist at the surface of polymeric NPs. The lowering of zeta potential value upon CBA conjugation was reasoned to be due to subsequent replacement of –COO group with terminal amine (NH_2) groups after protein conjugation[51]. The elevated magnitude of zeta potential offers repulsive inter-particle interaction preventing aggregation of the nanoparticles[52].

3.3.2. Entrapment Efficiency

MTX-NPs showed appreciably higher entrapment efficiency (79.9±2.4%) as compared to the CBA conjugated NPs (71.3±1.8%) (Table 1). Dissolution and subsequent loss of surface adhered MTX from MTX-NPs upon addition of NPs in the medium may be ascribed to the divergence in entrapment efficiency. These outcomes are consistent to the results obtained in earlier investigations[53].

View Article Online
DOI: 10.1039/C6RA17290C

3.4. *In vitro* drug release profile

In vitro drug release in pH 7.4 and 5.4 on plain and conjugated NPs demonstrated a biphasic drug release pattern suggesting an early burst, followed by a lag phase and a later apparent-zero order phase (Fig. 4C). MTX release of 20.26±1.58% and 28.9 ±2.45% was attained from CBA-MTX-NPs and MTX-NPs correspondingly in the PBS (pH 7.4). On the other hand, 21.4±1.03% and 33.9 ±1.15% of MTX was found to be released from CBA-MTX-NPs and MTX-NPs, respectively in the acidic media (pH 5.4) until the end of 8thh (Fig. 4C). The most probable reason that may be accounted to this rapid release of MTX can be accounted to the release of drug adsorbed on the surface of NPs. Furthermore, at pH 7.4, the cumulative MTX release from CBA-MTX-NPs and MTX-NPs was 73.51±3.64% and 88.3±4.85%, respectively at the end of 144 h. In other case, 95.60±3.53of MTX was found to be released from CBA-MTX-NPs at the end of 144 h. The extended release could be ascribed to the diffusion of drug molecules across the polymeric milieu of the NPs. However, a sizeable decrease in cumulative release of MTX from their CBA conjugated formulations was observed in comparison to their unconjugated counterparts at both pH values (pH 7.4 and pH 5.4). This may be ascribed to the structural integrity conferred by CBA, therefore providing a diffuse double layer obstacle and offering a steric hindrance to diffusion of drug[9,54].Furthermore, accelerated degradation of PLGA and lessening of ionic interaction between drug and PLGA at an acidic pH might be accountable for faster drug release at lower pH. Acidic pH catalyzes the cleavage of ester linkages in the polymer backbone and augments the erosion of polymeric matrix [55]. As a result, PLGA NPs could be anticipated to afford a pH-stimulating release of entrapped MTX at acidic milieu of tumor and might facilitate ligand mediated transcytosis as well.

3.5. *Ex vivo* studies

3.5.1. Cytotoxicity and cell uptake studies

The cytotoxic response in term of % growth inhibition of free MTX, MTX-NPs and CBA-MTX-NPs was evaluated by SRB assay against C-6 glioma cells. Percent Cellular inhibition response against all formulation was found to be concentration dependent. None of the formulation showed any effect on the survival of cells when the MTX equivalent concentration was below 1 μM, and in all these cases the cell viabilities were found to be well above 90% survival rate (Fig. 5 A, B & C).

View Article Online
DOI: 10.1039/C6RA17290C

Experiments conducted on xenografts model undoubtedly exemplify a dose dependent cytotoxic response that is a decrease in % cell survival with increase in concentration of drug. Nearly100 % of the cells were killed when concentration of MTX was 100 μM in case of all the formulation. Probably, the cytotoxic action of drug depends upon adequate access of drug in the cell and not merely by its presence in the adjacent milieu of a cell over the incubation period (72 h). In concentration range (1–100 μM) of MTX, the cytotoxic effect was sort out as CBA-MTX-NPs > MTX-NPs > CBA+ CBA–MTX-NPs > MTX (Fig. 5 A, B & C).

Maximum intracellular entry of CBA-MTX-NPs was conferred upon CBA conjugation via adsorption mediated endocytosis. Consequently, extended release of MTX leads to considerable higher cytotoxic action as compared to free MTX or MTX-NPs. The cytotoxic effects *via* MTX-NPs were measured less than CBA appended NPs possibly due to their entry in absence of any active transport mechanism and is mediated merely by passive diffusion mechanism. Furthermore, the nano metric size of the NPs may lead to the enhanced permeation and retention (EPR) effect and coating of CBA enhanced the adsorption as well as cell permeability due to changes in cell membrane fluidity. Besides, the %cellular inhibition was found significantly less when cells were incubated with CBA-MTX-NPs + CBA (1 mg/ml). This may be credited to the competitive inhibition of CBA functionalized NPs with free CBA. Free CBA was preferentially up taken by the cells, and therefore little entry of CBA-MTX-NPs was observed. The results are lined up with previous outcomes reported by Storm et al., 2002[56].

3.5.2. Cellular Uptake Study

Imperatively CBA-MTX-NPs facilitates higher cytotoxic response in C-6 cells, *in vivo* the ligand anchored formulation would promptly experience transcytosis therefore evading the possibility of marked increase in % cellular uptake effect on C-6 cells as compared to unconjugated formulation and fluorescence marker alone.

The efficacy of cellular uptake as a function of CBA conjugation and incubation time was determined using flow cytometry. Two h post incubation of plain FITC, FITC labeled MTX-NPs, FITC labeled CBA-MTX-NPs, and free CBA + FITC labeled CBA-MTX-NPs, the percent fluorescencein C-6 glioma cells was found to be 9.8 ± 2.4%, 14.1 ± 3.1%, 33.6 ± 3.3%, and 11.7 ± 3.2%, respectively (Fig. 5 D). Fluorescence intensity augmented with time ($p \leq 0.05$), which was merely 32.7±2.6%, 51.5±3.2%, 78.6±3.8%, and 39.6±3.3%, respectively after 6 h. The higher uptake of CBA conjugated formulation was possibly due to CBA residues tethered on the

View Article Online
DOI: 10.1039/C6RA17290C

facade of NPs when compared to unconjugated NPs ($p < 0.05$). This foremost cellular localization maybe credited to the adsorption mediated endocytosis mechanism facilitated by CBA. Furthermore, FITC alone and FITC labeled MTX-NPs illustrated fluorescence due to diffusion/endocytosis/phagocytosis mediated non-specific adsorption onto cell surfaces. In contrast incubation of free CBA along with FITC labeled CBA-MTX-NPs led to distinctly restrict entry into the tumor cell lines. This may be ascribed to competitive inhibition of CBA tethered NPs with free CBA. Free CBA preferentially gained access into the cells, and thus little entry of FITC labeled CBA-MTX-NPs was evaluated. The outcomes are lined up with previous studies [56].

3.6. *In vivo* pharmacokinetic and biodistribution studies

Biodistribution studies were carried out to examine the efficacy of CBA conjugated NPs in the delivery of anticancer agents to target tumor tissues while circumventing the BBB and also bypass peripheral tissues (kidney, heart, liver, etc.). Following injection of MTX entrapped in NPs, the initial maximum concentration attained was slightly lower than plain MTX (Fig. 6A).

After 2 h of administration, the content of MTX when injected as plain solution in kidney, liver, heart, spleen, and tumor tissues was 31.81 ± 1.41 µg/g, 10.13 ±0.97 µg/g, 5.3±0.7 µg/g, 8.1±0.87 µg/g, and 2.9±0.4 µg/g, respectively (Fig. 6A). The information evidently advocates the utmost NPs uptake by liver/spleen (organs rich in cells of RES) and access to the kidney, which is primary organ for its clearance. A nominal concentration of MTX was estimated in brain, the BBB acts as a main obstacle for delivery and further significantly impedes therapeutic effectiveness. Furthermore, the concentration of MTX declined rapidly in all the organs being untraceable in kidney and brain following 24 h of administration. This designates rapid removal/elimination/metabolism of drug from the body when administered in its original form.

On the contrary, after 24 h of formulation administration, the concentrations of MTX loaded in MTX-NPs were estimated to be: 11.51±1.09, 7.22±0.97, 3.31±0.91, 6.95±0.1.25 and 51.7±3.4 µg/g in the liver, kidney, heart, spleen and tumor, respectively (Fig. 6A). In the case of CBA conjugated NPs formulations, 112.69±6.41 µg/g of MTX was found in tumor tissues, 9.19±0.95 µg/g in the liver with a less amount in the heart and 5.1±0.57 µg/g in kidneys, and 5.63±0.49 µg/g in the spleen after 24 h (Fig. 6A). Sufficient amount of MTX was detected in liver and spleen following administration of MTX as MTX-NPs, and may be ascribed to the

View Article Online
DOI: 10.1039/C6RA17290C

uptake of polymeric particles by mononuclear phagocytic system. A slight access of MTX concentration in brain tissues was also observed. An improved residence time of MTX in the systemic circulation was also noted upon incorporation of MTX inside NPs that facilitated the redistribution process of drug into various tissues. Despite, deficiency of a targeting entity in case of MTX-NPs leads to non-selective/ non-specific distribution and thus the effect was not prominent.

The amount of MTX determined in kidney, liver, heart, spleen, and brain tissues was 6.03±0.39 µg/g, 9.24±0.76 µg/g, 0.94±0.04 µg/g, 8.03±1.01 µg/g and 19.89 ± 1.16 µg/g, respectively following 2 h administration of CBA-MTX-NPs (Fig. 6A). Importantly, after 2 h the MTX concentration with CBA-MTX-NPs in brain was increased by 39.26 and 2.17 folds when compared to free MTX and MTX-NPs. The outcomes undoubtedly advocate the targeted delivery of MTX to brain with CBA decorated NPs. This may be ascribed to CBA tethering that make possible to NPs to pass across the BBB by adsorption mediated transcytosis [27,28]. The stratagem may also facilitate enlarge the therapeutic efficacy by providing possibility to diminish the dose of bioactive moieties and drug incorporated delivery vehicles.

Circulation life time, plasma profile as well as therapeutic effectiveness of MTX was enormously altered after entrapment of MTX inside nanoparticles and upon conjugation of CBA. Plasma profiles of various MTX formulations after single i.v. injection in Balb/c mice were demonstrated in Fig 6B. Concentration of MTX in serum after i.v. administration of free MTX was estimated to be 1.57±0.052 µg/ml, after 30 min and 0.13±0.039 µg/ml after 24 hrs. This steep decrease might be due to the rapid elimination of MTX from the kidneys and instantaneous distribution in various organs. Conversely, after administration of the MTX loaded nanoparticles formulation, the concentration of MTX in serum was significantly low. The maximum concentration of MTX estimated in the serum following 12 h was calculated to be 1.11±0.047 and 1.19±0.087 µg/ml for MTX-NPs and CBA–MTX–NPs respectively. Though, 0.27±0.041 and 0.68±0.71 µg/ml of MTX was measured in the plasma until the end of 24 and 20 h following administration of CBA-MTX-NPs and MTX-NPs, respectively (Fig. 6B). The outcomes merely signify the long circulation characteristic of NPs while ligand tethered formulation having the extended residence time. Concentration of MTX in serum was sustained to a greater extent in case of CBA-MTX-NPs than that of MTX-NPs probably due to the double barrier effect to drug diffusion upon surface modification with CBA[54]. The information offered to this point merely

View Article Online
DOI: 10.1039/C6RA17290C

imply CBA-MTX-NPs have noticeably enhanced bioavailability and apparently extended retention in systemic circulation and the result could not be accomplished via pre-treatment of mice with MTX-NPs or plain MTX.

3.7. Hemolytic toxicity

Concentration at 0.1 μM (equivalent of MTX), free MTX exhibited 17.9±0.6% hemolysis; however, MTX-NPs and CBA–MTX-NPs formulations displayed 11.7±0.3%, and 6.1±0.51% hemolysis, respectively (Fig. 6C). The toxicity of polymeric NPs was not as much of in comparison to free MTX due to the incorporation of drug in a biocompatible nanostructured milieu. However, the hemolytic toxicity of NPs with functionalities at the surface is a major limitation in the use of such systems and was adequate to exclude its use as vehicles for drug delivery. CBA anchored to the NPs surface appreciably diminishes the hemolysis of the RBCs certainly due to inhibition of communication of RBCs with the anticancer moiety associated with the surface of MTX-NPs.

4. Conclusions

NPs are the biocompatible nano-carriers which have been expansively investigated for the delivery of therapeutics. This is the first report of its own kind that offers an insight to use of cationic bovine serum albumin tethered biodegradable polymeric nanostructured carriers for brain tumors exploiting adsorption mediated transcytosis to circumvent the highly lipophilic BBB. The present study discloses CBA functionalized polymeric nanoparticles as proficient vectors to carry large doses of anti-cancer drug for its sustained and targeted delivery. CBA tethered NPs incorporating MTX demonstrated cytotoxicity higher than that of plain MTX on C-6 glioma cells at all the concentration tested. The formulation proficiently navigated huge doses of anti-cancer therapeutic agent across the BBB. The best promising therapeutic response and diminution in annoying side effects may be facilitated by site specific delivery strategy. Nevertheless, meticulous exercises require to be carried out to attain any unambiguous generalization.

Ethical Statement

All animal studies were conducted in accordance with current legislation of institute on animal experiments, and protocol was approved by the 'Institutional Animal Ethical Committee' of Dr. Hari Singh Gour University, Sagar (M.P. India). Animals were maintained in climatically controlled rooms and fed with standard rodent food pellet (Lipton India Ltd, Bombay) and water

View Article Online
DOI: 10.1039/C6RA17290C

ad libitum. The study was carried out with the guidelines of Council for the Purpose of Control and Supervision of Experiments on Animals (CPCSEA), Ministry of Social Justice and Empowerment, Government of India.

Acknowledgements

The authors are grateful for a grant and fellowship provided by the AICTE, New Delhi and Council of Scientific and Industrial Research (CSIR, HRDG), New Delhi, India.

References

1 Y. L. Koo, G. R. Reddy, M. Bhojani, R. Schneider, M. A. Philbert, A. Rehemtulla, B. D. Ross and R. Kopelman, 2006, **58**, 1556–1577.

2 N. Dwivedi, J. Shah, V. Mishra, M. C. I. Mohd Amin, A. K. Iyer, R. K. Tekade and P. Kesharwani, *J. Biomater. Sci. Polym. Ed.*, 2016, **27**, 557–80.

3 A. Agarwal, U. Gupta, A. Asthana and N. K. Jain, *Biomaterials*, 2009, **30**, 3588–3596.

4 L. Juillerat-jeanneret, 2008, **13**.

5 L. Juillerat-Jeanneret, *Drug Discov. Today*, 2008, **13**, 1099–106.

6 L. Prokai and K. Prokai-Tatrai, Eds., *Peptide Transport and Delivery into the Central Nervous System*, Birkhäuser Basel, Basel, 2003.

7 Y. Persidsky, S. H. Ramirez, J. Haorah and G. D. Kanmogne, *J. Neuroimmune Pharmacol.*, 2006, **1**, 223–36.

8 V. K. Venishetty, R. Komuravelli, M. Kuncha, R. Sistla and P. V Diwan, *Nanomedicine*, 2013, **9**, 111–21.

9 A. Jain, A. Jain, N. K. Garg, R. K. Tyagi, B. Singh, O. P. Katare, T. J. Webster and V. Soni, *Acta Biomater.*, 2015, **24**, 140–151.

10 V. Mishra and P. Kesharwani, *Drug Discov. Today*, 2016, **21**, 766–78.

11 A. Béduneau, P. Saulnier and J.-P. Benoit, *Biomaterials*, 2007, **28**, 4947–67.

12 M. D. Chavanpatil, A. Khdair, Y. Patil, H. Handa, G. Mao and J. Panyam, *J. Pharm. Sci.*, 2007, **96**, 3379–3389.

13 M. O. Oyewumi and R. J. Mumper, *Int. J. Pharm.*, 2003, **251**, 85–97.

14 A. Gothwal, P. Kesharwani, U. Gupta, I. Khan, M. C. Iqbal Mohd Amin, S. Banerjee and A. K. Iyer, *Curr. Pharm. Des.*, 2015, **21**, 4519–26.

15 P. Kesharwani, V. Mishra and N. K. Jain, *J. Drug Deliv. Sci. Technol.*, 2015, **28**, 1–6.

16 N. P. Praetorius and T. K. Mandal, *Recent Pat. Drug Deliv. Formul.*, 2007, **1**, 37–51.

17 K. Gao and X. Jiang, *Int. J. Pharm.*, 2006, **310**, 213–219.

18 T. Yoshikawa, T. Sakaeda, T. Sugawara, K. Hirano and V. J. Stella, *Adv. Drug Deliv.*

View Article Online
DOI: 10.1039/C6RA17290C

Rev., 1999, 36, 255–275.

19 N. Nasongkla, E. Bey, J. Ren, H. Ai, C. Khemtong, J. S. Guthi, S. F. Chin, A. D. Sherry, D. A. Boothman and J. Gao, *Nano Lett.*, 2006, **6**, 2427–2430.

20 I. V Larina, B. M. Evers, T. V Ashitkov, C. Bartels, K. V Larin and R. O. Esenaliev, *Technol. Cancer Res. Treat.*, 2005, **4**, 217–226.

21 P. Kesharwani, S. Banerjee, S. Padhye, F. H. Sarkar and A. K. Iyer, *Biomacromolecules*, 2015.

22 P. Kesharwani, L. Xie, S. Banerjee, G. Mao, S. Padhye, F. H. Sarkar and A. K. Iyer, *Colloids Surf. B. Biointerfaces*, 2015, **136**, 413–423.

23 M. Thöle, S. Nobmann, J. Huwyler, A. Bartmann and G. Fricker, *J. Drug Target.*, 2002, **10**, 337–44.

24 U. Bickel, T. Yoshikawa and W. M. Pardridge, *Adv. Drug Deliv. Rev.*, 2001, **46**, 247–79.

25 Y.-L. Xie, W. Lu and X.-G. Jiang, *Behav. Brain Res.*, 2006, **173**, 76–84.

26 A. Agarwal, A. Asthana, U. Gupta and N. K. Jain, *J. Pharm. Pharmacol.*, 2008, **60**, 671–88.

27 W. Lu, Q. Sun, J. Wan, Z. She and X.-G. Jiang, *Cancer Res.*, 2006, **66**, 11878–87.

28 W. Lu, Y.-Z. Tan, K.-L. Hu and X.-G. Jiang, *Int. J. Pharm.*, 2005, **295**, 247–60.

29 V. P. Torchilin, *Nat. Rev. Drug Discov.*, 2005, **4**, 145–60.

30 R. Misra and S. Mohanty, *J. Mater. Sci. Mater. Med.*, 2014, **25**, 2095–2109.

31 S. B. Kaye, *Br. J. Cancer*, 1998, **78 Suppl 3**, 1–7.

32 L. Costantino, F. Gandolfi, G. Tosi, F. Rivasi, M. A. Vandelli and F. Forni, *J. Control. Release*, 2005, **108**, 84–96.

33 Y. Cui, Q. Xu, P. K.-H. Chow, D. Wang and C.-H. Wang, *Biomaterials*, 2013, **34**, 8511–20.

34 Q. T. H. Shubhra, J. Tóth, J. Gyenis and T. Feczkó, *Colloids Surf. B. Biointerfaces*, 2014.

35 R. Singh, P. Kesharwani, N. K. Mehra, S. Singh, S. Banerjee and N. K. Jain, *Drug Dev. Ind. Pharm.*, 2015, 1–14.

36 K. C. Song, H. S. Lee, I. Y. Choung, K. I. Cho, Y. Ahn and E. J. Choi, *Colloids Surfaces A Physicochem. Eng. Asp.*, 2006, **276**, 162–167.

37 D. R. Nogueira, L. Tavano, M. Mitjans, L. Pérez, M. R. Infante and M. P. Vinardell, *Biomaterials*, 2013, **34**, 2758–72.

38 A. K. Jain, A. Jain, N. K. Garg, A. Jain, S. A. Jain, R. K. Tyagi and G. P. Agrawal, *Colloids Surfaces B Biointerfaces*, 2014.

39 D. Bhadra, S. Bhadra, S. Jain and N. K. Jain, *Int. J. Pharm.*, 2003, **257**, 111–124.

40 L. Tavano, R. Muzzalupo, L. Mauro, M. Pellegrino, S. Ando, N. Picci and A. Rende,

View Article Online
DOI: 10.1039/C6RA17290C

2013.

41 N. K. Garg, G. Sharma, B. Singh, P. Nirbhavane and O. P. Katare, *J. Liq. Chromatogr. Relat. Technol.*, 2015, **38**, 1629–37.

42 P. Kesharwani, S. Banerjee, S. Padhye, F. H. Sarkar and A. K. Iyer, *Colloids Surfaces B Biointerfaces*, 2015.

43 X. Ying, H. Wen, W.-L. Lu, J. Du, J. Guo, W. Tian, Y. Men, Y. Zhang, R.-J. Li, T.-Y. Yang, D.-W. Shang, J.-N. Lou, L.-R. Zhang and Q. Zhang, *J. Control. Release*, 2010, **141**, 183–92.

44 M. W. Amjad, M. C. I. M. Amin, H. Katas, A. M. Butt, P. Kesharwani and A. K. Iyer, *Mol. Pharm.*, 2015, **12**, 4247–4258.

45 S. Valable, E. L. Barbier, M. Bernaudin, S. Roussel, C. Segebarth, E. Petit and C. Rémy, *Neuroimage*, 2007, **37 Suppl 1**, S47–58.

46 A. E. Gulyaev, S. E. Gelperina, I. N. Skidan, A. S. Antropov, G. Y. Kivman and J. Kreuter, *Pharm. Res.*, 1999, **16**, 1564–1569.

47 P. Kesharwani, R. K. Tekade and N. K. Jain, *Pharm. Res.*, 2015, **32**, 1438–1450.

48 K. Avgoustakis, A. Beletsi, Z. Panagi, P. Klepetsanis, A. G. Karydas and D. S. Ithakissios, *J. Control. Release*, 2002, **79**, 123–135.

49 K. J. Kim and Y. Byun, *Biotechnol. Bioprocess Eng.*, 1999, **4**, 210–214.

50 A. Agarwal, S. Majumder, H. Agrawal, S. Majumdar and G. P. Agrawal, *Curr. Nanosci.*, 2011, **7**, 71–80.

51 A. Agarwal, H. Agrawal, S. Tiwari, S. Jain and G. P. Agrawal, *Int. J. Pharm.*, 2011, **421**, 189–201.

52 A. Jain, P. Kesharwani, N. K. Garg, A. Jain, S. A. Jain, A. K. Jain, P. Nirbhavane, R. Ghanghoria, R. K. Tyagi and O. P. Katare, *Colloids Surfaces B Biointerfaces*, 2015.

53 A. Jain, A. Agarwal, S. Majumder, N. Lariya, A. Khaya, H. Agrawal, S. Majumdar and G. P. Agrawal, *J. Control. Release*, 2010, **148**, 359–67.

54 V. Soni, D. V. Kohli and S. K. Jain, .

55 B. S. Zolnik and D. J. Burgess, 2007, **122**, 338–344.

56 P. B. Storm, J. L. Moriarity, B. Tyler, P. C. Burger, H. Brem and J. Weingart, *J. Neurooncol.*, 2002, **56**, 209–17.

View Article Online
DOI: 10.1039/C6RA17290C

Table captions:

Table 1: Zeta Potential, Particle Size, PDI and %Drug Entrapment of nano-formulations.

Figure captions:

Fig.1: FT-IR spectra of (A) BSA, (B) CBA and (C) CBA-MTX-NPs.

Fig. 2: NMR of (A) CBA and (B) CBA-MTX-NPs.

Fig.3: Particle size of (A) MTX-NPs and (B) CBA-MTX-NPs. Zeta potential of (A) MTX-NPs and (B) CBA-MTX-NPs.

Fig.4: (A and B) SEM image of CBA-MTX-NPs and (C) In vitro release profile of MTX from MTX-NPs and CBA-MTX-NPs in PBS (pH 7.4) and PBS (pH 5.4). Inset graph represents the drug release at the initial time points. Each data point represents mean ± SD (n = 6).

Fig.5: Cell cytotoxicity of Plain MTX, MTX-NPs, CBA-MTX-NPs and CBA+CBA-MTX-NPs (A) after 24 h, (B) after 48 h and (C) after 72 h. (D) Cellular uptake efficiency of plain FITC, FITC labeled MTX-NPs, FITC labeled CBA-MTX-NPs and CBA+ FITC labeled CBA-MTX-NPs in C-6 glioma cells. Each data point represented as mean ± SD (n = 4).

Fig.6: (A) Biodistribution of Plain drug and formulations attained at various time intervals in different tissues (n=6; $p \leq 0.05$*, [a]). *Significant difference between free MTX Vs MTX-NPs and CBA-MTX-NPs, [a] significant difference between MTX-NPs and CBA-MTX-NPs. (B) Serum concentration of MTX attained at various intervals (n=6; $p \leq 0.05$*,[a]). *Significant difference between free MTX Vs MTX-NPs and CBA-MTX-NPs, [a] significant difference between MTX-NPs and CBA-MTX-NPs. (C) Comparative hemolytic toxicity study (n=6; $p \leq 0.05$*, [a]). *Significant difference between free MTX Vs MTX-NPs and CBA-MTX-NPs, [a] significant difference between MTX-NPs and CBA-MTX-NPs.

View Article Online
DOI: 10.1039/C6RA17290C

Table 1: Zeta Potential, Particle Size, PDI and %Drug Entrapment of nano-formulations.

Formulation Code	Zeta Potential (mV)	Particle Size (nm)	PDI	%Drug Entrapment
MTX-NPs	-13.7± 0.4	108.3±3.1	0.015±0.004	79.9±2.4%
CBA- MTX-NPs	-5.55± 0.3	120.9±4.4	0.155±0.007	71.3±1.8%

Results are presented as Mean ± SD (n=3)

View Article Online
DOI: 10.1039/C6RA17290C

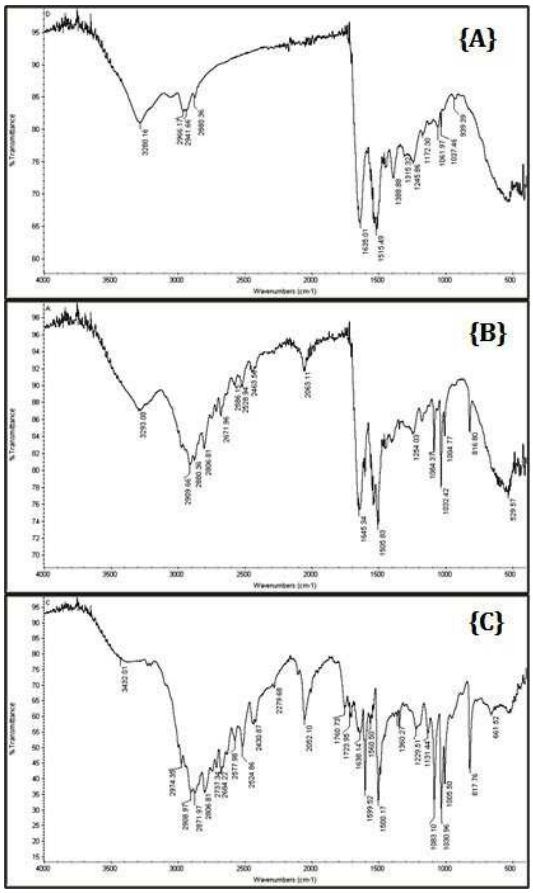

Fig.1: FT-IR spectra of (A) BSA, (B) CBA and (C) CBA-MTX-NPs.

View Article Online
DOI: 10.1039/C6RA17290C

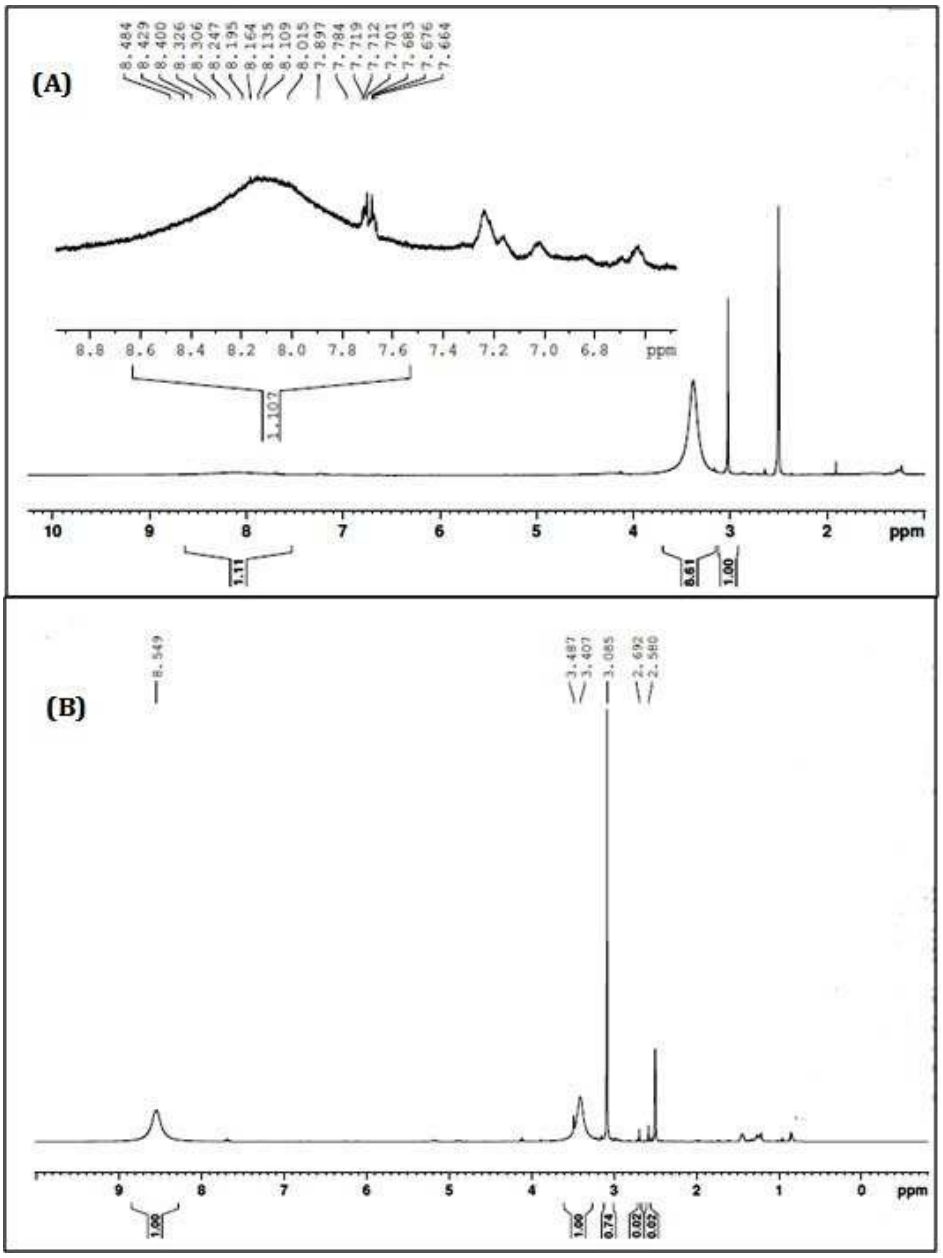

Fig.2: NMR of (A) CBA and (B) CBA-MTX-NPs.

View Article Online
DOI: 10.1039/C6RA17290C

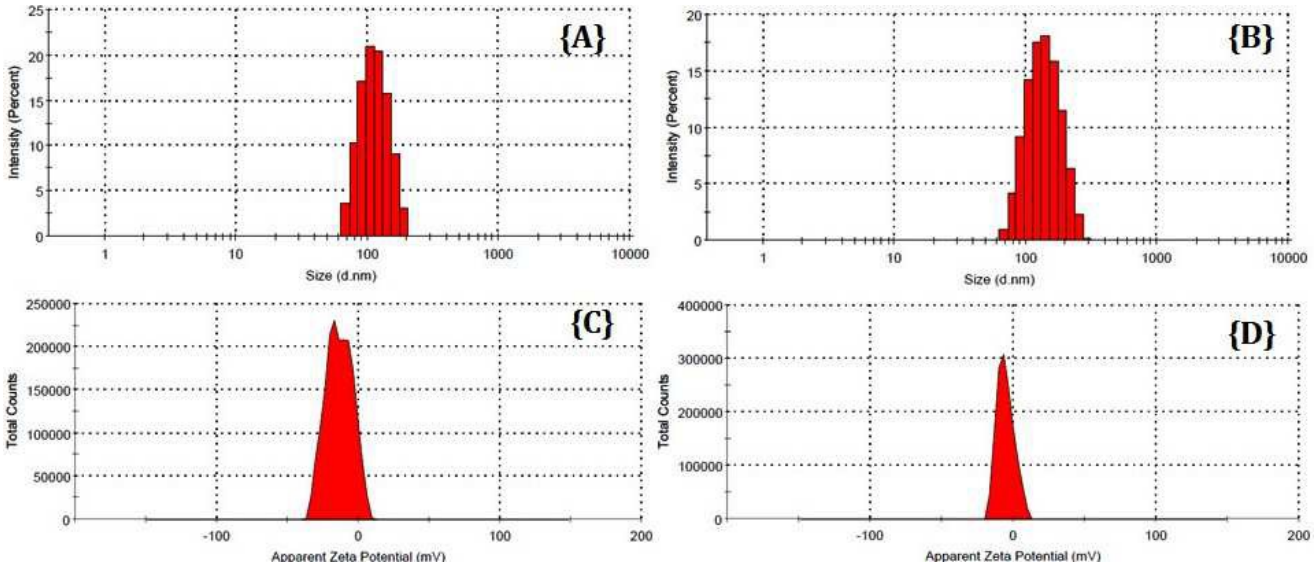

Fig.3: Particle size of (A) MTX-NPs and (B) CBA-MTX-NPs. Zeta potential of (A) MTX-NPs and (B) CBA-MTX-NPs.

View Article Online
DOI: 10.1039/C6RA17290C

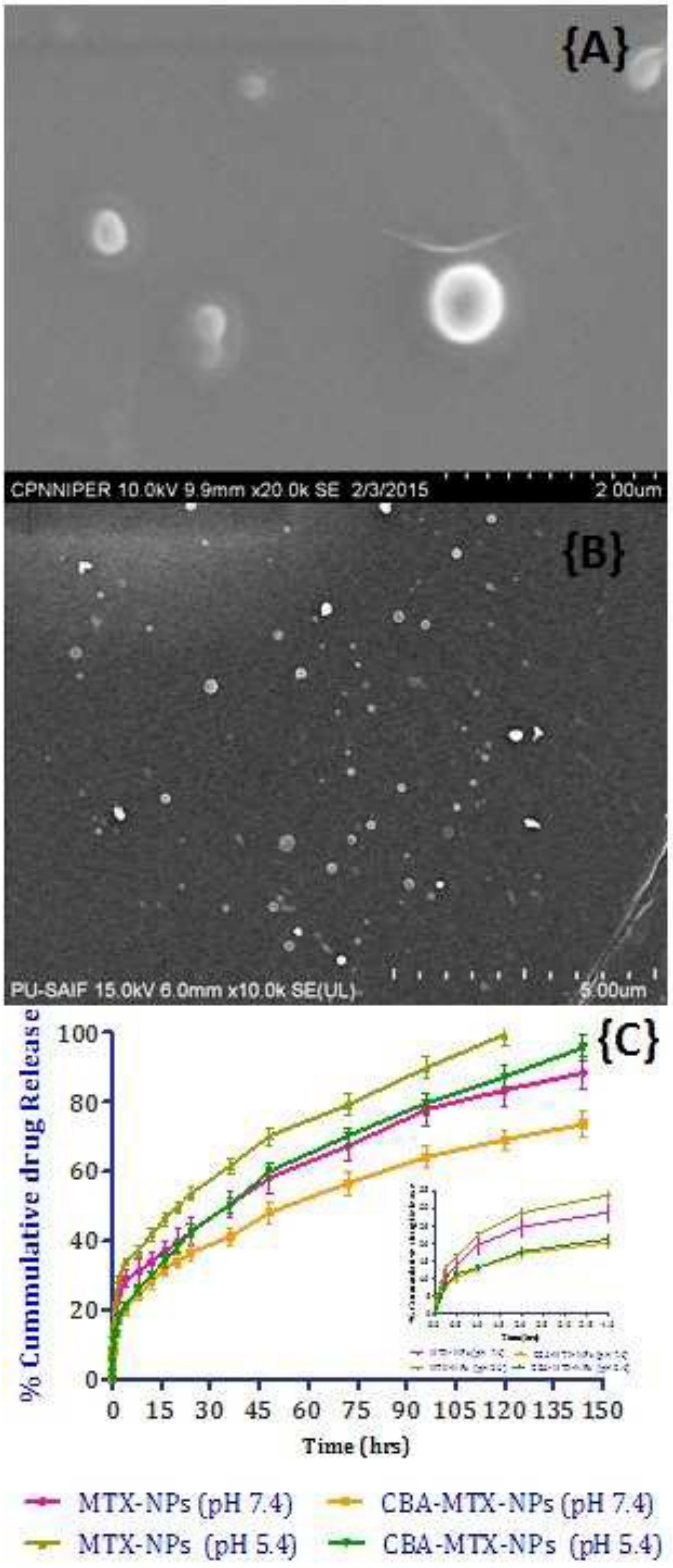

Fig.4: (A and B) SEM image of CBA-MTX-NPs and (C) In vitro release profile of MTX from MTX-NPs and CBA-MTX-NPs in PBS (pH 7.4) and PBS (pH 5.4). Inset graph represents the drug release at the initial time points. Each data point represents mean ± SD (n = 6).

View Article Online
DOI: 10.1039/C6RA17290C

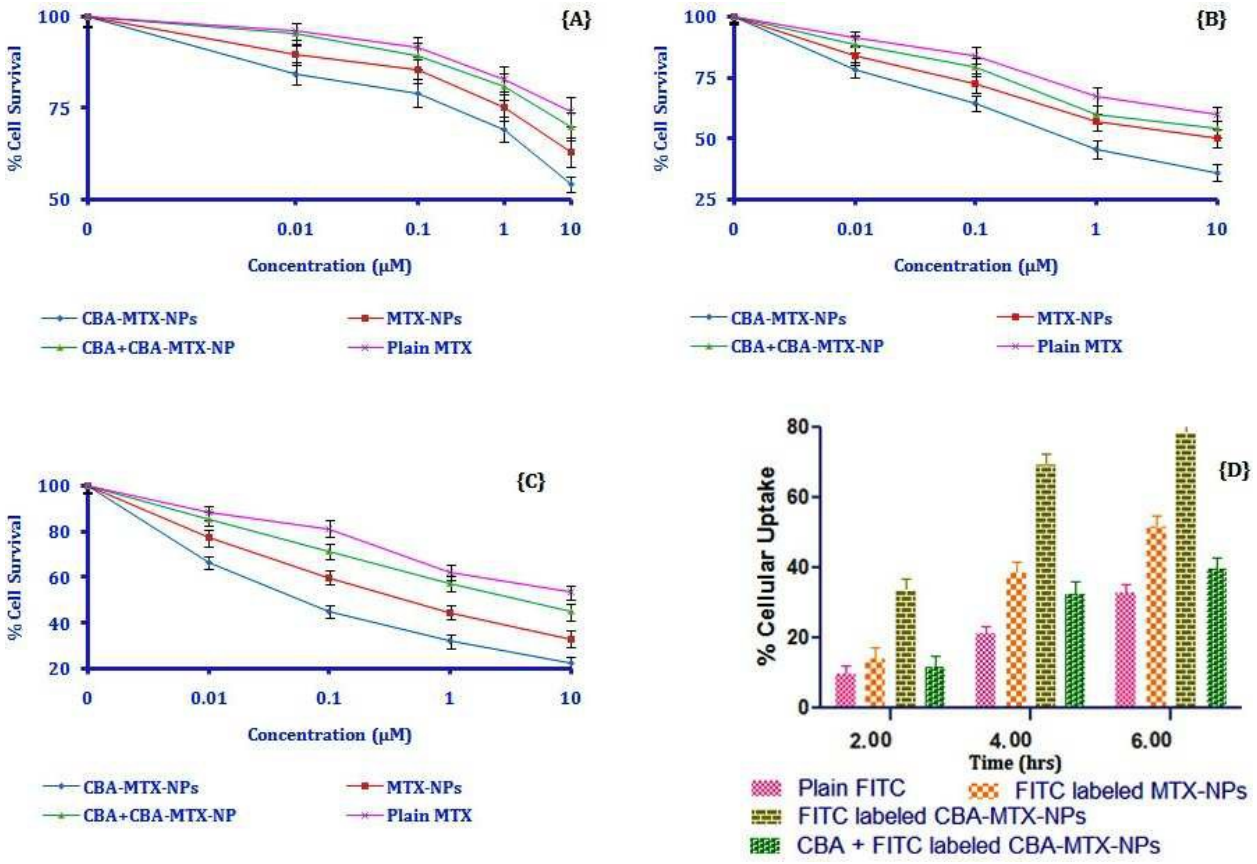

Fig.5: Cell cytotoxicity of Plain MTX, MTX-NPs, CBA-MTX-NPs and CBA+CBA-MTX-NPs (A) after 24 h, (B) after 48 h and (C) after 72 h. (D) Cellular uptake efficiency of plain FITC, FITC labeled MTX-NPs, FITC labeled CBA-MTX-NPs and CBA+ FITC labeled CBA-MTX-NPs in C-6 glioma cells. Each data point represented as mean ± SD (n = 4).

View Article Online
DOI: 10.1039/C6RA17290C

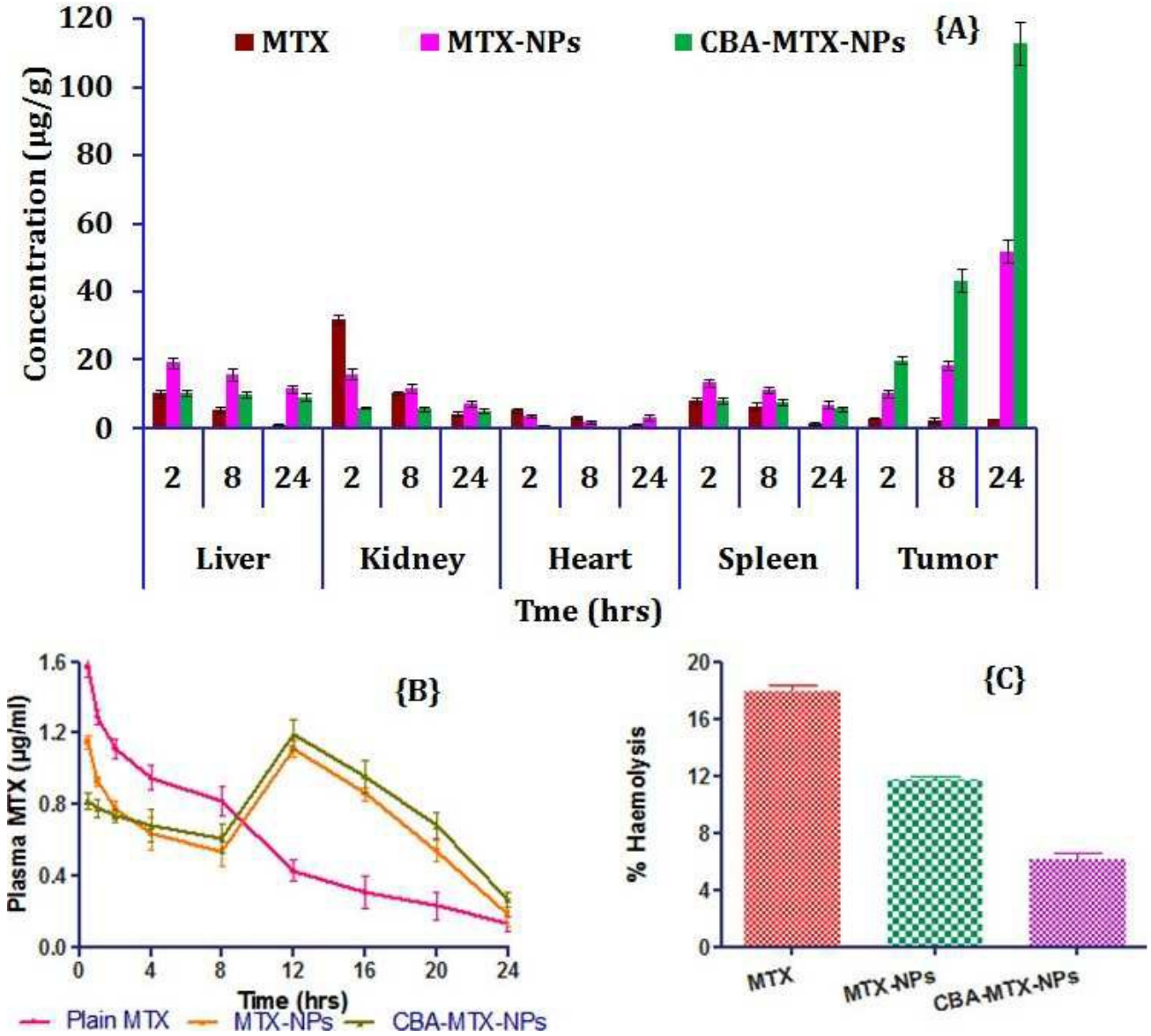

Fig.6: (A) Biodistribution of Plain drug and formulations attained at various time intervals in different tissues (n=6; $p \leq 0.05$*, [a]). *Significant difference between free MTX Vs MTX-NPs and CBA-MTX-NPs, [a]significant difference between MTX-NPs and CBA-MTX-NPs. (B) Serum concentration of MTX attained at various intervals (n=6; $p \leq 0.05$*,[a]). *Significant difference between free MTX Vs MTX-NPs and CBA-MTX-NPs, [a] significant difference between MTX-NPs and CBA-MTX-NPs. (C) Comparative hemolytic toxicity study (n=6; $p \leq 0.05$*, [a]). *Significant difference between free MTX Vs MTX-NPs and CBA-MTX-NPs, [a]significant difference between MTX-NPs and CBA-MTX-NPs.